ORDEM DOS ENGENHEIROS
INFORMAÇÃO GEOESPACIAL PARA AS GERAÇÕES FUTURAS
OPORTUNIDADES E DESAFIOS
VIII CNCG
CONFERÊNCIA NACIONAL DE CARTOGRAFIA E GEODESIA
29 e 30 de outubro de 2015

Spatio-temporal variability of the wet component of the troposphere

Eliana VIEIRA[1,*], Clara LÁZARO[1,2] e M. Joana FERNANDES[1,2]

[1] Faculdade de Ciências, Universidade do Porto
[2] Centro Interdisciplinar de Investigação Marinha e Ambiental (CIIMAR)

(up200806838@fc.up.pt; clazaro@fc.up.pt; mjfernan@fc.up.pt)

Keywords: Wet Path Delay, Satellite Altimetry, Spatio-temporal Variability

Abstract: The wet component of the troposphere is due to the presence of water vapor and cloud liquid water in the atmosphere and is responsible by a delay in the propagation of the altimeter signals (Wet Path Delay, WPD), less than the delay due to the dry component. However, due to the high variability of the water vapor distribution, both in space and time, this component is one of the main error sources in Satellite Altimetry.

The WPD can be obtained from on-board microwave radiometer (MWR) measurements with centimetric precision in open-ocean. However, the WPD retrieval is hampered by the contamination of the surrounding lands and ice in the radiometer measurements, leading to a rejection or loss of accuracy in the altimetric measurements.

The main objective of this work is the study of the space-time variability of the wet component of the troposphere in global terms. WPD was computed using TCWV (Total Column Water Vapor) and t2m (two-meter temperature) products provided by ERA Interim atmospheric model were used. These WPD products are latitude-longitude grids of monthly mean WPD values with a spatial resolution of 0.75ºx0.75º, for the period of 25 years since January 1, 1990 until December 31, 2014. The Seasonal and Trend decomposition (STL) procedure was used to derive both the seasonal and trend components aiming at study the contribution of these components to the variability of WPD. Results show maximum values of variance along the Equator and over the intertropical zone e.g. in Southern and Eastern Asia, Northern Australia, Central Africa, Southwestern United States of America, and Southern Africa. The variability of WPD has a strong dependency on latitude and is related to the temperature and to Climate phenomena found in these regions. Seasonal component has a strong contribution on WPD variability, mainly in the Northern Hemisphere with a contribution of almost 100%.

Global and hemispherical time-series of monthly means of WPD values, weighted according to their associated latitude, were generated and analyzed. The temporal analysis shows that, adjusting a linear fit to the trend component of the three time-series, the largest slope is about 0.1 mm /year.

The temporal correlation of WPD with SLA (Sea Level Anomaly) and with various climate patterns (e.g. Niño 3.4 and SOI (Southern Oscillation Index)), responsible for abnormal weather conditions, is presented. Since the oceans provide the primary reservoir for atmospheric water vapor and the source of precipitation is evaporation of seawater, this study can contribute to a better understanding of the hydrologic cycle variability and climate change.

1. Introduction

Satellite Altimetry aims at estimating the long-term sea level with an accuracy of a few cm. Although, corrections to the altimetric radar measurements are needed to accomplish this aim. These measurements are affected by external perturbations. The atmosphere reduces the speed of the radar pulse, bending its trajectory and, therefore, causing a "path delay" of the altimeter signal. This effect of the atmospheric refraction is due to the two components of the troposphere, hydrostatic (or dry) and wet, and to the existence of free electrons in the upper atmosphere. Given the small difference between the hydrostatic and dry components of the tropospheric path delay, the term "dry tropospheric delay" is usually used within the altimetry community to refer to the hydrostatic tropospheric path delay (Fernandes et al., 2014).

The aim of this work is the study of one of the components of the delay, the wet component. This delay is caused by the presence of water vapor and cloud liquid water in the atmosphere, and is a relatively small, but difficult to estimate, error source, due to the variability of the water vapor and to its fast change in space and time. Studies about the mean and standard deviation of WTC (Wet Tropospheric Correction), using observations of column water vapor from 6 years of Jason-1 data, reveals that the WTC has significant temporal and spatial variability (Andersen and Scharroo, 2011). Corrections for this component can be determined using passive measurements from on-board microwave radiometers (MWR) or by using meteorological parameters from atmospheric models. The two most widely used models are the European Centre for Medium-Range Weather Forecasts (ECMWF) and the U.S. National Centers for Environmental Prediction (NCEP). Both are delivered on regular grids at regular 6-hour intervals.

The wet tropospheric path delay can also be measured on the ground (using GNSS or upward looking radiometers) and then compared to the one derived from the on-board microwave radiometers (Fernandes et al., 2014).

The wet tropospheric correction (WTC) from the on-board microwave radiometers is hampered by the contamination on the radiometer measurements closed to ice or land areas, making it usable only in Open Ocean. This sensitivity of the correction to land and ice contamination as well as to instrument malfunction in certain epochs has been the aim of recent studies, (see e.g. Fernandes et al., 2013, Fernandes et al., 2014, Desportes et al., 2007).

A methodology for the computation of improved wet delay values for all contaminated, and therefore prone to be rejected, values were created at the University of Porto (U. Porto) in the aim of ESA financed projects (GNSS-Path Delay Plus, GPD+). Based on this methodology, enhanced products were generated globally for the eight main altimetric missions: ERS-1/2, Envisat, T/P, Jason-1/2, CryoSat-2 e SARAL (Fernandes et al., 2015).

It is well-known that most wet tropospheric models are not suitable for processing long time series of satellite altimetry since they possess long-term errors and discontinuities. A comparison between the various methodologies to generate the wet delay can be found in Obligis et al. (2011).

For studies over inland water Fernandes et al. (2014), recommended that the MWR-derived WTC should be adopted whenever available, or the GNSS-derived WTC in regions possessing GNSS permanent stations. In the absence of the previous data types the adoption of a model-derived correction from ERA-Interim, computed at surface height, provide the highest accuracy (1-3 cm). Over ocean, the most suitable corrections are the GPD+ WTC (Fernandes et al., 2015).

For use in satellite altimetry, the WTC can be calculated from global grids of two single-level parameters provided by global atmospheric models, such as the ERA-Interim model, the total column water vapor (TCWV, usually expressed in kg/m^2 or millimeters (mm), as the length of an equivalent column of liquid water) and near-surface air temperature (two-meter temperature t2m expressed in Kalvin (K), also referred in this article as T_0), from the following expression (Bevis et al., 1994):

$$WTC = -\left(0.101995 + \frac{1725.55}{T_m}\right)\frac{TCWV}{1000} \quad (1)$$

where T_m is the mean temperature of the troposphere, which can be modelled from T_0, according to, e.g., (Mendes *et al.*, 2000):

$$T_m = 50.440 + 0.789T_0 \quad (2)$$

Equations (1) and (2) provide the WTC at the level of the atmospheric model orography.

Since the WTC has always negative values, the symmetric value of WTC will be assumed and analyzed, the WPD (Wet Path Delay). Given that WTC is expressed in meters (m), and its values are in the order of centimeters, a reduction to centimeters (cm) is needed allowing a better interpretation of the results presented in this work.

In order to compute WPD using meteorological parameters, the ERA-Interim model was used. ERA-Interim is a global atmospheric reanalysis project produced by the ECMWF (European Centre for Medium-Range Weather Forecasts). It covers the period since January 1, 1979 and provides gridded data products that include a large variety of 3-hourly surface parameters, describing weather as well as ocean-wave and land-surface conditions, and 6-hourly upper-air parameters covering the troposphere and stratosphere. The data provided by the ECMWF server allows computing WPD all over the world (Dee et al., 2011).

The main goal of this work is the study of the variability of WPD in space and time. The data used in this work are described in Section 2.

Section 3 presents the spatial analysis, where the variability of WPD is described and how seasonal and trend components contribute to this variability. Global and hemispherical time-series of monthly means of WPD values, weighted according to their associated latitude, were generated and analyzed in section 4. The variables in study have impact on climate, being the source of important climate patterns. Section 5 presents results for the correlation of WPD and Climate Indices (e.g. Darwin SLP (Sea level Pressure), allowing to identify some causes of the WPD variability in certain areas. Section 6 presents another also but important relationship to check: the relationship between WPD and SLA (Sea Level Anomaly) – the correlation between these two variables will show how WPD can contribute to sea level changes, which is an important result in Satellite Altimetry. Finally, conclusions of the work are presented in Section 7.

2. Data used

According to Equations (1) and (2), the variables needed to calculate the WPD are the t2m (2-meter temperature) and the TCWV (Total Column Water Vapor). These data products were extracted from the server of ECMWF (http://apps.ecmwf.int/datasets/data/interim_full_daily/. The gridded data products were generated using 0.75ºx0.75º latitude-longitude grids, since January 1, 1990 until December 31, 2014, covering a 25-year period. The Spatial and Temporal analysis, the correlation with Climate Indices and the correlation with SLA uses these data.

The Earth System Research Laboratory (ESRL) - Physical Sciences Division (PSD) conducts weather and climate research to observe and understand Earth's physical environment, and to improve weather and climate predictions on global-to-local scales. PSD provides Monthly Atmospheric and Ocean Time-Series about Teleconnections, Atmosphere, Precipitation, ENSO (El Niño Southern Oscillation), SST (Sea Surface Temperature) and others (http://www.esrl.noaa.gov/psd/data/climateindices/list/), and the National Weather Service – Climate Prediction Center (http://www.cpc.ncep.noaa.gov/data/indices) provides monthly atmospheric data such as SLP (Sea Level Pressure) from Darwing, Australia, allowing to compute the correlation between WPD and Climate Indices. Data were used for the same period of the WPD, over 25 years.

SLA (Sea Level Anomaly) gridded data were provided by the ESA Climate Change Initiative Sea Level (SL/cci) project. Data are sampled monthly using 0.25ºx0.25º latitude-longitude grids, since January 1, 1993 until December 15, 2013, covering a 20-year period.

3. Spatial analysis

3.1. WPD variability

Most of the water vapor is in the troposphere and increases with increased temperature, and the greatest amount of water vapor is found near the equator (Thurman and Burton, 2001). The general decrease of water vapor from equator to poles is a reflection of the global distribution of temperature, because warm air is capable of holding more moisture than cold air. There are exceptions in the major desert regions, where the air is very dry despite its high temperature.

Studies of the water vapor distribution in different regions around the world, including Europe, America, Africa, and Asia, allowed concluding that the distribution of water vapor changes with seasonal changes in temperature and atmospheric circulation patterns (Seidel, 2002). Therefore, WPD variability study is important, once WPD depends on the variability of water vapor and temperature.

To conduct this study, the variance and RMS (Root Mean Square) statistical measures were chosen, while the first is related to the standard-deviation, the second is related with the mean of WPD (or, more precisely, the first is the square of the standard-deviation

and the second is the square root of mean of the values of WPD). Therefore, the variance and RMS of WPD was calculated for each grid point, along the period of study (Figure 1 and 2, respectively).

According to Figure 1, the variance of WPD has a strong dependency on latitude, as Andersen and Scharoo (2011) demonstrated from Jason-1 data, studying the mean and standard deviation of the wet tropospheric correction. The highest values of WPD variance are found in areas closed to the tropic of Cancer and closed to the tropic of Capricorn (~23º 30' N and 23º 30' S respectively). Maximum variance values of WPD are found over the intertropical zone e.g. in Southern and Eastern Asia, Northern Australia, Central Africa, Southwestern United States of America, and Southern Africa. Other regions namely Mexico and the southwest USA, and parts of South America and South Africa also reveal high values for variance of WPD.

The lowest variation is found closed to Antarctica with a value between 0 and 5 cm^2.

The RMS values of WPD (Figure 2) show a near-zonal dependency, with absolute values ranging from less than 5 cm at high latitudes to ~35 cm near the equator and the tropics. Therefore, WPD values are higher near to equator and decreases from equator to Polar Regions. These results match with WPD measurements and water vapor distributions.

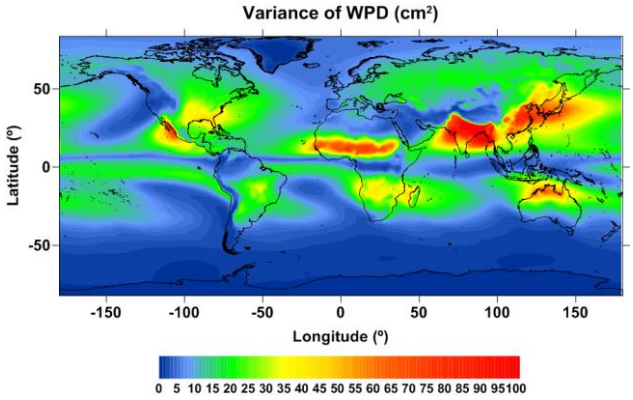

Figure 1 – Spatial distribution of the Variance of WPD

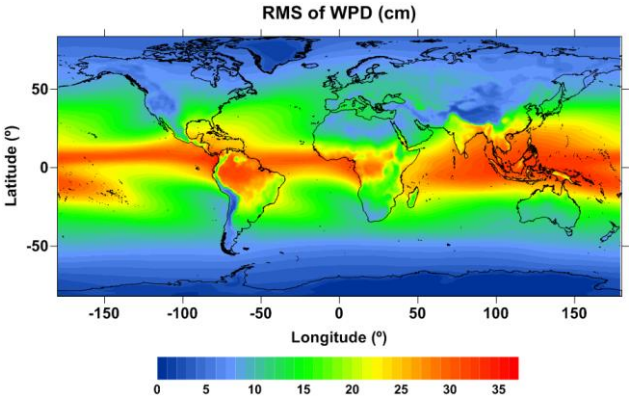

Figure 2 – Spatial distribution of RMS of WPD

3.2. Seasonal and Trend Components

For each grid point, the corresponding time-series was decomposed into seasonal and trend components using the Seasonal and Trend Decomposition using Loess (STL) filtering procedure (Cleveland et al., 1990). The parameters used to apply the STL decomposition were the same for all time-series presented in this study. In this study, trend is the component that describes data variations with a period longer than 1½ year; the seasonal component has a period of 12 observations; the seasonal parameter is set for a smoothing window spanning 13 observations and the trend parameter is set for a window covering 21 observations.

The variance values of the seasonal component are estimated at each grid point, allowing the calculation of the relative contribution of this component to the variance of WPD (shown in Figure3), given by the determination coefficient (DC) equation (3) (Volkov and Aken, 2003):

$$DC_{component} = \frac{\sigma^2_{component}}{\sigma^2_{WPD}} \times 100\% \quad (3)$$

The spatial distribution of the determination coefficient of the season component, Figure 3, shows that the variance of the seasonal component is the principal contribution for the variance of WPD in the Northern Hemisphere. Besides the seasonal patterns in Indian Ocean due to monsoon, and the Advection Fog found in California, the seasonal pattern of South Pacific also contributes to the variability of WPD, since there is a hotter and more humid period in Summer, and a cooler and drier period during Spring (Thurman and Burton, 2001). It is clear that in the Equator line this contribution varies between 15% and 50%, increasing towards Polar Regions. However, the contribution of the variance of the Trend component has the opposite behavior (Figure 4). In the areas of the largest contribution of the seasonal component, the trend component contributes less and vice-versa. Comparing the contributions of the seasonal and trend components with the variance of WPD, it is possible to conclude that in the areas of the largest variability, the seasonal component contributes almost 100%, whereas the trend component has almost 0% of contribution.

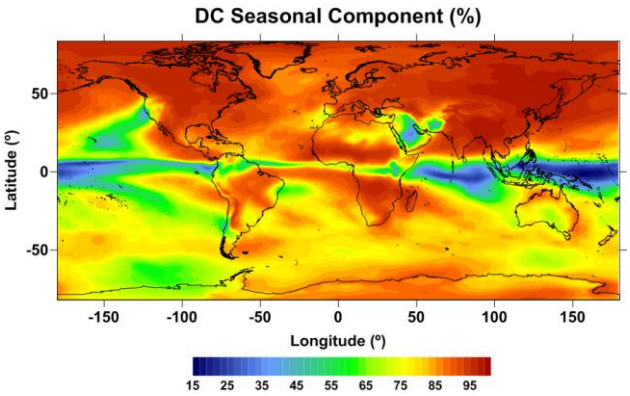

Figure 3 – Spatial distribution of the Determination Coefficient of the Seasonal component of WPD.

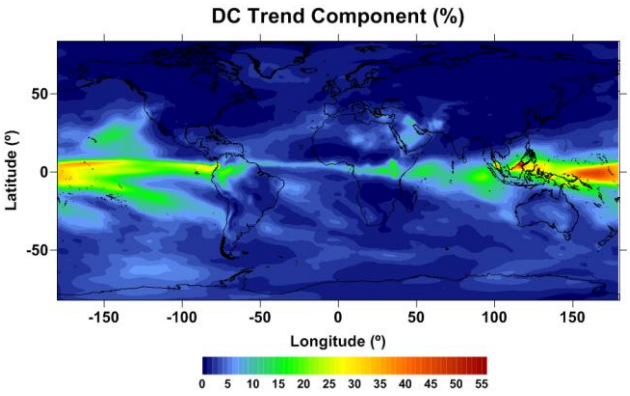

Figure 4 – Spatial distribution of the Determination Coefficient of the Trend component of WPD.

4. Temporal analysis

The temporal analysis consists on studying the Global and hemispherical time-series of monthly means of WPD values, weighted according to their associated latitude. The global time-series of WPD and the corresponding seasonal and trend time-series, from STL decomposition, are shown in Figure 5. The time-series of WPD (top panel) clearly shows the effect of the seasonal component. The seasonal component has an average peak-to-peak amplitude of 1.98 cm. The trend component of the time-series explains how the WPD varies with time, ignoring the seasonal periodicity. Adjusting a linear fit to the trend component the observed slope has a value of 0.09 mm/year. A previous study about Northern Hemisphere reveals slopes for annual and interannual components of water vapor in the troposphere at different regions. Pacific is the region with the highest slope, with values upper than 1.14 mm/decade (Ross and Elliott, 2000).

The same analyses were done for the North and South hemispheres, see Figure 6. The WPD time-series allows concluding that the global time-series is influenced by the difference in phase between both hemispheres.

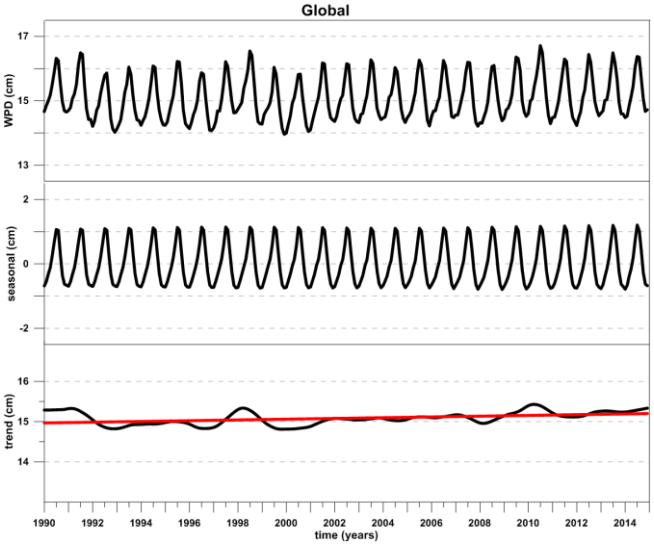

Figure 5 – STL decomposition for the Global time-series. WPD time-series (top-panel); Seasonal Component (middle-panel); Trend component with linear fit represented with red colour (bottom-panel)

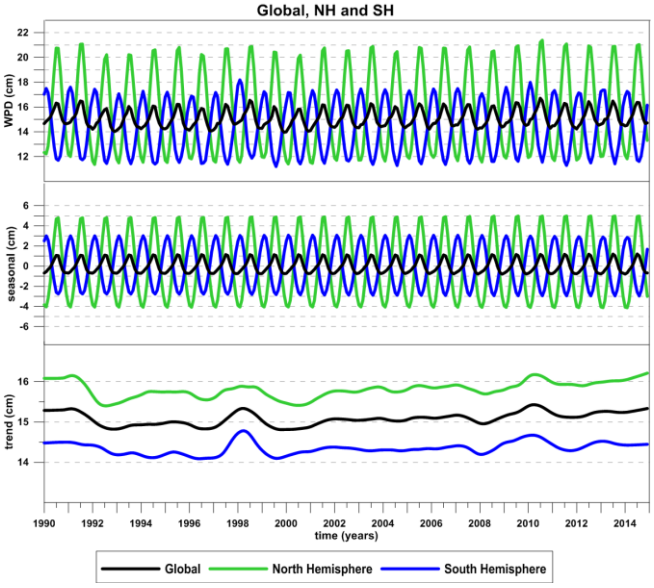

Figure 6 – STL decomposition of Global, and hemispherical time-series. WPD time-series (top-panel); Seasonal Component (middle-panel); Trend (bottom-panel)

Concerning the averaged WPD time-series for the analyzed time-series, the mean and the standard deviation of WPD present the highest values over the North Hemisphere, and the lowest values over the South hemisphere. The maximum values of WPD are found over the North hemisphere. These results are expected since the Northern Hemisphere has more land, with lower heat capacity than the ocean, it shows faster temperature, and water vapor, changes. As with temperature, seasonal changes in water vapor appear to be stronger in the northern hemisphere than in the southern hemisphere (Seidel, 2002). Adjusting a linear fit to the trend component of each time-series, see Figure 6 (bottom panel), it is possible to conclude that the coefficient of determination (R^2) has values smaller than 0.3, which means that the model of adjustment only explains the values observed in 30%. The highest slopes found are in order of 0.1 mm/year. When comparing the trend components of the three time-series it is clear that the maximum and minimum values occur at the same epochs.

5. Correlation with Climate Indices

Correlation exists when two variables have a linear relationship beyond what is expected by chance alone. It is important to know how WPD is related with some Climate Indices. In this work Climate Indices related to SST (sea surface temperature) were used, such as ONI (Oceanic Niño Index), Niño 1+2, Niño 3, Niño 3.4 and Niño 4, TNA (Tropical Northern Atlantic Index) and TSA (Tropical Southern Atlantic Index), with AMO (Atlantic Multidecadal Oscillation) and Darwin SLP (Sea Level Pressure from Darwin, Australia). These Climate Indices were chosen because WPD depends on temperature, as described in previous sections, and pressure is also related to temperature because decreases more rapidly with altitude where the air is cold, and is known that temperature in the lower troposphere generally decreases from the subtropics to the Polar Regions (Thurman and Burton, 2001). Each grid point of WPD was correlated with each time-series of Climate Indices. Figure 7 presents plots with the spatial distribution of the correlation coefficients for each case. The white areas indicate no statistical significance at the 5% level.

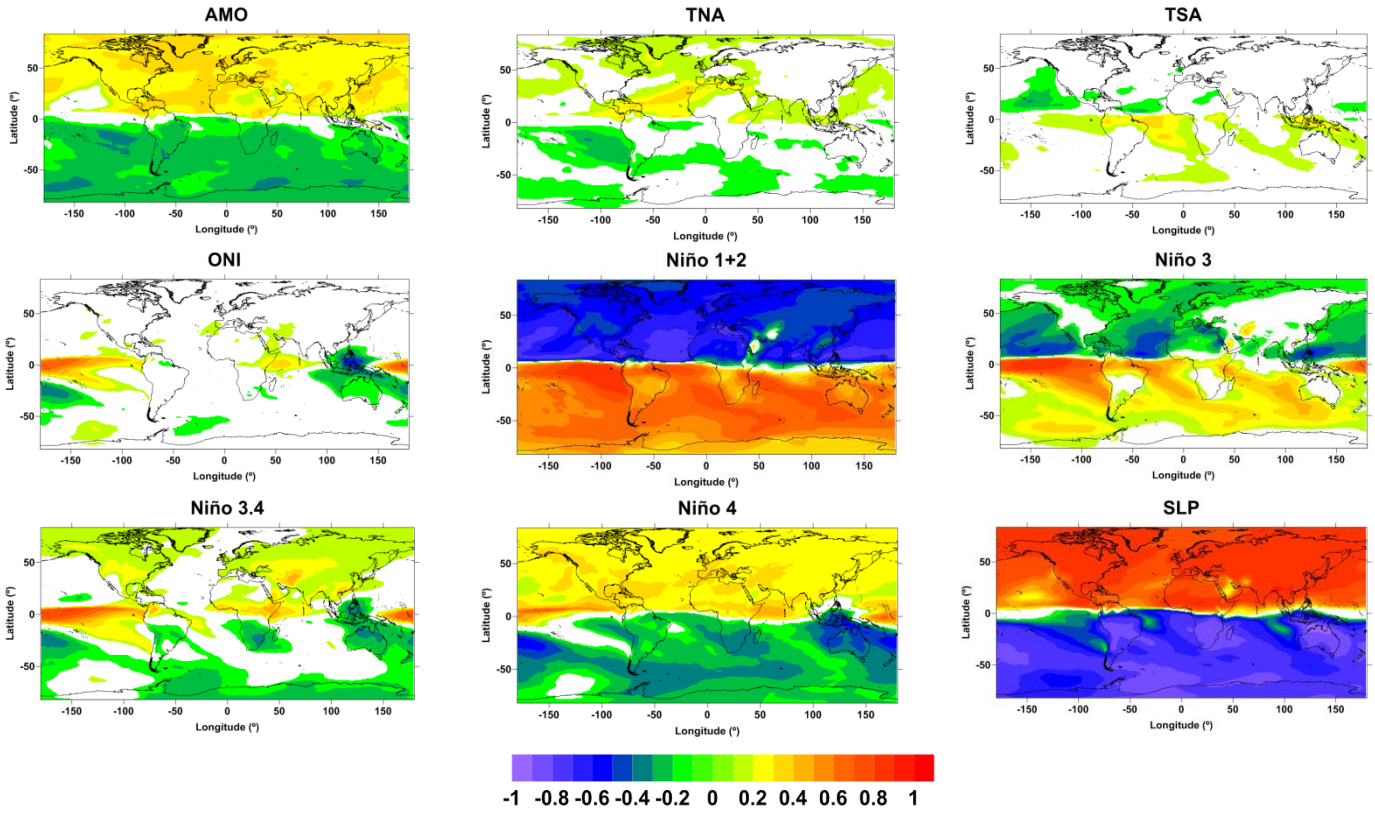

Figure 7 – Correlation Coefficient of WPD and Climate Indices. White indicates no statistical significance at the 5% level

Results show that WPD is highly related with El Niño phenomenon, and there is a less and almost none relation with AMO, TSA and TNA indices since the correlation coefficient is close to 0. The spatial distribution of the correlation coefficient of SLP with WPD reveals that in the Northern Hemisphere when Darwin SLP increases WPD increases and in the Southern Hemisphere when Darwin SLP increases WPD decreases. The relation between Niño 1+2 and WPD shows that in Northern Hemisphere, when WPD increases Niño 1+2 decreases and, in Southern Hemisphere when WPD increases also Niño 1+2 increases.

6. Correlation with SLA

Since the study of Sea Level is very important in Satellite Altimetry, the knowledge of how related WPD is with Sea Level Anomalies (SLA) is also important. Each grid point of WPD was correlated with the respective grid point of SLA. The spatial distribution of the correlation coefficient between WPD and SLA, Figure 8, shows that near to coast of Southern Asia, the variables are highly related but with a negative coefficient, which means that when SLA increases, WPD decreases. The same relation is found near North of Brazil, in the Equatorial Counter Current. Following this current to Africa the correlation coefficient takes positive and high values, which means that WPD increases with SLA. In the remaining areas, the most frequent values for the correlation coefficient are between 0.3 and 0.7, so it relation can exist in these cases or not.

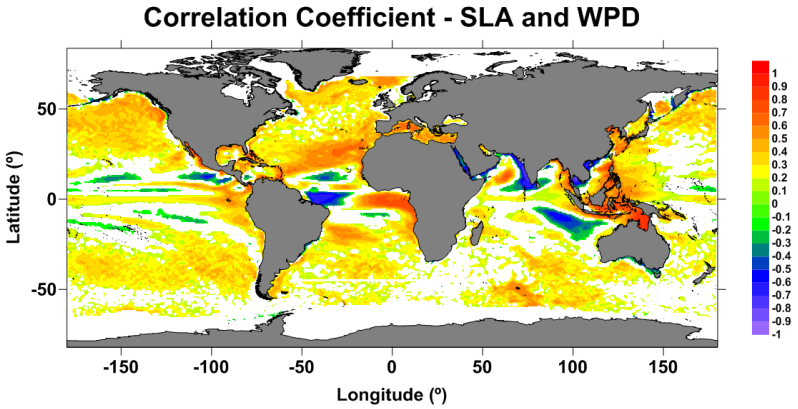

Figure 8 – Correlation Coefficient of WPD and SLA. White represents invalid areas or areas with no statistical significance at the 5% level

7. Conclusions

This study allows understanding the variability of the distribution of the Wet Path Delay. Considering the period since January 1, 1990 until December 31, 2014, it is possible to conclude that WPD variability has a strong dependency on latitude, since the maximum variance values for WPD are found in the Northern Hemisphere. Climate Phenomena are the cause for this high variability, since they affect the water vapor and temperature over the intertropical zone e.g. in Southern and Eastern Asia, Northern Australia, Central Africa, Southwestern United States of America, and Southern Africa. The seasonal component of WPD is related to the seasonal patterns presented in these regions and in the Southern Pacific, and contributes almost 100% to the variance of WPD. The trend component has a maximum contribution of 55% in the equatorial line, where the contribution of the seasonal component decreases.

The analysis of the Global and hemispherical time-series of WPD allows estimating that WPD is increasing with time by approximately 0.1 mm per year. The maximum and minimum values for the trend component occur in the same areas. The global time-series is influenced by the difference in phase between both hemispheres.

Since WPD variability can be related to atmospheric and ocean events, the correlation with Climate Indices and with SLA is very important. The temporal correlation of WPD with various Climate Indices shows that WPD is highly related with El Niño phenomenon, and with Darwin SLP. In the Northern Hemisphere when Darwin SLP increases, WPD increases, the reverse process happening in the Southern Hemisphere. The analysis of the correlation between WPD and SLA allows identifying areas where SLA is related to WPD, such as near the coast of Southern Asia, North of Brazil in the Equatorial Counter Current.

References

Aguado E., Burt J. E. (2001). Understanding Weather and Climate, Second Edition, Prentice Hall pp. 81

Andersen, O. B.; Scharoo, R. (2011), Range and Geophysical Corrections in Coastal Regions: And Implications for Mean Sea Surface Determination. In Coastal Altimetry; Vignudelli, S., Kostianoy, A.G., Cipollini, P., Benveniste, J., Eds.; Springer-Verlag: Berlin/Heidelberg, Germany, pp. 113–116.

Bevis, M., Businger, S., Chiswell, S., Herring, T.A., Anthes, R.A., Rocken, C., Ware, R.H. (1994). GPS meteorology—Mapping zenith wet delays onto precipitable water. J. Appl. Meteorol. 33, 379–386.

Cleveland, R.B., Cleveland, W.S., McRae, J.E., Terpenning, I. (1990). STL: a seasonal-trend decomposition procedure based on loess. J. Offshore Stat. 6, 3–73.

Dee, D.P., Uppala, S.M., Simmons, A.J., Berrisford, P., Poli, P., Kobayashi, S., Andrae, U., Balmaseda, M.A., Balsamo, G.; Bauer, P., et al. (2011), The ERA-Interim reanalysis: Configuration and performance of the data assimilation system. Q. J. R. Meteorol. Soc., 137, 553–597.

Desportes, C., Obligis, E., Eymard, L. (2007). On the wet tropospheric correction for altimetry in coastal regions. IEEE Trans. Geosci. Remote Sen., 45, 2139–2149.

Fernandes M. J., Lázaro C., Ablain M., Pires N. (2015). Improved wet path delays for all ESA and reference altimetric missions, Remote Sensing of Environment. http://dx.doi.org/10.1016/j.rse.2015.07.023

Fernandes, M. J., Lázaro, C., Nunes , A. L., Scharroo, R. (2014). Atmospheric Corrections for Altimetry Studies over Inland Water, Remote Sens, 6, 4952-4997

Fernandes, M.J., Pires, N., Lázaro, C., Nunes. (2013). Tropospheric delays from GNSS for application in coastal altimetry. Adv. Space Res, 51, 1352–1368.

Mendes, V.B., Prates, G., Santos, L., Langley, R.B. (2000). An Evaluation of the Accuracy of Models of the Determination of the Weighted Mean Temperature of the Atmosphere. In Proceedings of the ION 2000 National Technical Meeting, Anaheim, CA, USA, 26–28.

Obligis, E., Desportes, C., Eymard, L., Fernandes, M.J., Lázaro, C., Nunes, A.L. (2011), Tropospheric Corrections for Coastal Altimetry. In Coastal Altimetry; Vignudelli, S., Kostianoy, A.G., Cipollini, P., Benveniste, J., Eds.; Springer-Verlag: Berlin/Heidelberg, Germany, pp. 147–176.

Ross R. J., Elliott W. P. (2000). Radiosonde-Based Northern Hemisphere Tropospheric Water Vapor Trends, Journal of Climate, Vol.4

Seidel, D. J. (2002). Water Vapor: Distribution and Trends. Encyclopedia of Global Environmental Change.

Thurman H. V., Burton E. (2001). Introductory Oceanography, Nine Edition, Prentice Hall.

Volkov, D. L., Aken H.M. (2003), Annual and interannual variability of sea level in the northern North Atlantic Ocean. Journal of Geophysical Research., 108 (C6), 3204, doi:10.1029/2002JC001459.